

Self-interference between forward and backward propagating parts of a single acoustic plate mode

M. Germano, A. Alippi, M. Angelici, and A. Bettucci

Department of Energetics, University of Rome "La Sapienza," Via A. Scarpa 14, 00161 Rome,

Istituto Nazionale di Fisica della Materia, INFN, Sezione di Roma I Italy

(Received 21 November 2001; published 28 March 2002)

Near and far fields of a particular (S_1) Lamb mode, generated on a steel plate by means of a wedge transducer, are investigated. These show an oscillating behavior of the radial profile of the acoustic field amplitude that can be interpreted and modelled as interference phenomenon between forward and backward propagating parts of the Lamb mode, simultaneously generated at the interface between transducer and plate.

DOI: 10.1103/PhysRevE.65.046608

PACS number(s): 43.20.+g

I. INTRODUCTION

A clear evidence for the degeneracy of modes in coupled oscillators is the splitting of the energy levels, producing beating between degenerate modes [1]. In propagating waves, degeneracy sounds as a mystified concept, wouldn't it be for guided modes, where transverse conditions in the guide do localize energy, thus, setting on proper conditions for degeneracy. In the present paper, beating conditions are experimentally verified in the case of elastic plate perturbations that could be considered as degenerate, in as much as they correspond to waves that propagate with the same frequency, belong to the same mode but have different wave numbers. Experiments have been theoretically explained by considering the generation of two contradirected waves that, in a limited range of frequencies, belong to the same acoustic plate mode and whose energies flow into the same direction: the waves, of different amplitudes, interfere one with the other producing a stationary mode with finite standing wave ratio.

Both forward and backward propagating modes (Lamb modes) are a combination of shear and longitudinal waves that satisfy the stress-free conditions on the plate surfaces, whose dispersion curves can be found numerically by solving the so called Rayleigh-Lamb equation [2,3]:

$$\frac{\tan k_{ts}b}{\tan k_{tl}b} = - \left[\frac{4\beta^2 k_{ts}k_{tl}}{(k_{ts}^2 - \beta^2)^2} \right]^{\pm 1} \quad (1)$$

where + and - signs are used for symmetric and antisymmetric modes, respectively, $k_{ts}^2 = (\omega/v_s)^2 - \beta^2$ and $k_{tl}^2 = (\omega/v_l)^2 - \beta^2$ are the transverse wavenumbers for shear and longitudinal waves, respectively, with ω the angular frequency and β the component of the wavenumber along the direction of propagation. Both symmetric and antisymmetric modes are usually numbered by the nodal planes of the vibration amplitude between the plate-free surfaces. It can be found that, within a proper range of frequencies, S_1 dispersion curve has a negative slope such that a wave packet, properly generated, would have a phase velocity contradirected with respect to its group velocity [4]: this is called backward wave, to distinguish it from the usual forward one, and several interesting properties of it have been shown in the past [5-7]. Figure 1 represents the dispersion curve of S_1 mode both for positive and negative values of the wave vec-

tor. A horizontal line is drawn at a frequency value in the range where two backward wave packets (points B_1 and B_2) as well as two forward ones (points F_1 and F_2) exist. The subscripts 1 and 2 stand for the two directions where energy flows, two wave packets (B_1 and F_1) can be generated, at the very same frequency for such a mode, propagating (with group velocity) along direction 1 with their β vectors (phase velocities) contradirected. The same holds for direction 2.

II. EXPERIMENTAL EVIDENCE FOR SELF-INTERFERENCE

A wedge transducer with variable angle is used for generating Lamb modes [8]: the transducer area is 25.4×12.7 mm, and longitudinal waves, generated into a Lucite wedge support, impinge onto the surface of a 2-mm-thick homogeneous steel plate (AISI 304) with a variable angle of incidence. The radiating zone, given by the section of the field generated by the active transducer emitting surface, is a rectangular zone of size $a = 12.7/\cos \theta$ mm in the x direction and $b = 25.4$ mm in the y direction, with θ the angle between the impinging beam and the normal to the surface. At each selected angle of incidence there corresponds a specific value of the wave vector component β along the plate.

In the present case, a 10° angle and a frequency equal to 1.38 MHz have been chosen and a wave packet of $80 \mu\text{s}$ long has been generated. A couple of wave packets are generated along each direction: a backward packet B_1 together with a weaker forward packet F_1 in direction 1 and a for-

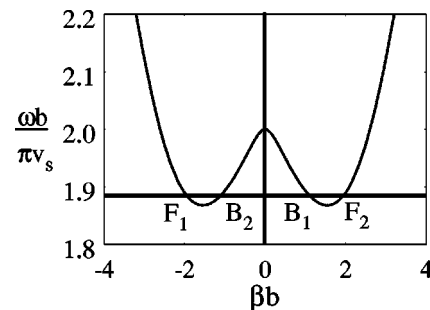


FIG. 1. Dispersion curve of the S_1 Lamb mode in adimensional units: at the frequency of 1.38 MHz (horizontal line), B backward and F forward modes are excited in directions 1 and 2. ($b = 0.002$ m, $v_s = 2920$ m/s).

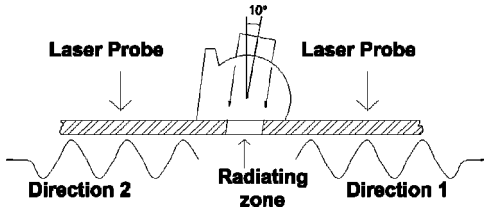


FIG. 2. Experimental setup.

ward packet F_2 with a weaker backward packet B_2 in the opposite direction 2. The relative intensities are due to the different efficiency in generating forward and backward wave packets for the two directions.

The acoustic field on the plate has been detected on both directions away from the wedge transducer, by means of a heterodyne laser interferometer that probes both the amplitude and phase of the vibration of the plate at different points of the surface with resolution of ≈ 1 mm (see Fig. 2).

Figure 3 (experimental curve) reports the vibration amplitude of the surface, detected with an acousto-optical probe, along the ultrasonic beam axis, on the rear side with respect to the wedge (direction 1). The detected amplitude decays along propagation direction, with oscillations about 10% around the mean value and an average wavelength of $\lambda_{\text{exp}} = 3.8$ mm. The wavelength of the central frequency wave has been measured by tracking its phase change while moving the probing spot along the propagation direction, it results to be $\lambda_b = 11.57$ mm as expected for a backward wave from the theoretical curve, the phase decreases as the laser spot is moved forward, thus, proving the contradirected nature of the backward wave. This case is interpreted as interference between B_1 and F_1 parts of the mode (see Fig. 1).

Figure 4 (experimental curve) reports the vibration amplitude, detected along direction 2: the oscillating behavior of the detected amplitude is present here, too, with the same average wavelength $\lambda_{\text{exp}} = 3.8$ mm, as in the previous case, while the wavelength of the central frequency wave resulting equal to $\lambda_f = 5.46$ mm as expected for a forward wave. The phase behavior, indeed, is a forward one. This case is interpreted as interference between F_2 and B_2 parts of the mode (see Fig. 1).

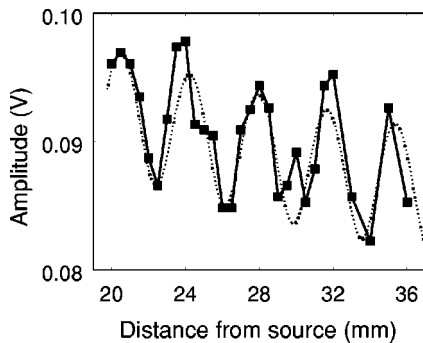


FIG. 3. Theoretical (dotted line) and experimental (squares) curves, of the amplitude profile vs distance from the source, along direction 1, where a backward wave packet interferes with a weaker forward wave packet.

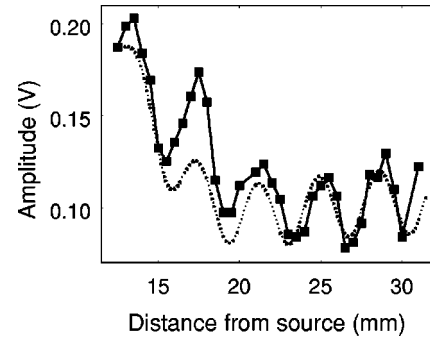


FIG. 4. Theoretical (dotted line) and experimental (squares) curves, of the amplitude profile vs distance from the source, along direction 2, where a forward wave packet interferes with a weaker backward wave packet.

III. THEORETICAL MODEL FOR SELF-INTERFERENCE

The previously reported data are explained by considering, for each direction, the interference between the backward wave having amplitude B and wave vector k_b with the forward wave having amplitude F and wave vector k_f propagating into opposite direction. The resulting field of the propagating waves is

$$\begin{aligned} f(x,t) &= \text{Re}[B e^{i(\omega t + k_b x)} + F e^{i(\omega t - k_f x)}] \\ &= \text{Re}[2F \cos(k_+ x) e^{i(\omega t - k_- x)} + (B - F) e^{i(\omega t + k_b x)}] \end{aligned} \quad (2)$$

with $k_+ = (k_f + k_b)/2$ and $k_- = (k_f - k_b)/2$. In this case, where no attenuation has yet been taken into consideration for either wave component, plotting the amplitude $\Phi(x_0) = \max[f(x_0, t)]$ of the field vs distance from the source x_0 , will simply result into a sinusoidally varying function, between values $|B + F|$ and $|B - F|$. In Fig. 5, the function $\Phi(x_0)$ is plotted showing that the amplitude modulation is actually due to a stationary wave with standing wave ratio $|(B + F)|/|(B - F)|$ and wavelength $\lambda_{\text{mod}} = \lambda_+/2 = \pi/k_+ = \lambda_b \lambda_f / (\lambda_b + \lambda_f)$. In fact, by considering the values λ_b

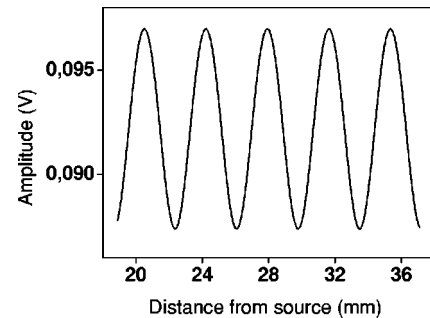


FIG. 5. Theoretical profile of the amplitude modulation function $\Phi(x_0)$ vs distance from source x_0 , along direction 1 (without considering decay due to diffraction effect), with $B_1 = 0.0922$ V and $F_1 = 0.0048$ V.

= 11.57 mm and $\lambda_f = 5.46$ mm, one has $\lambda_{\text{mod}} = 3.71$ mm, and this value agrees fairly well with the experimental data where oscillations have an average wavelength $\lambda_{\text{exp}} = 3.8$ mm.

The attenuation of the experimental curves (squares) in Figs. 3 and 4, is mainly due to diffraction from a finite width transducer. In order to take account of such effect, the field has been computed by Kirchhoff-Fresnel theory of the emission from a rectangular source along a perpendicular axes, central with respect to the acoustic field [9]. In case of direction 1, where $B_1 \gg F_1$, the field is mainly contributed by B_1 component, whose wavelength λ_b is such that experimental data are definitely in the Fraunhofer region, far from the last maximum of the Fresnel region, and the decay is slight, in

case of direction 2, where $F_2 \gg B_2$, the wavelength λ_f is such that measures are closer to the Fresnel last maximum, so that the slope of the decay is steeper. The final results for both directions are reported in Figs. 3 and 4, respectively, with a fair agreement between theoretical and experimental curves.

In conclusion, an interference effect has been reported between the forward and backward propagating part of the same acoustical plate mode, generated on a steel plate. Theoretical interpretation is given for the vibration amplitude distribution on the free surface, on both sides from the same emitting couple-mode transducer. Results are interpreted by taking into consideration the diffracting effect of the generated beams, as well.

-
- [1] P. M. Morse and K. U. Ingard, *Theoretical Acoustics* (McGraw-Hill, New York, 1968).
- [2] B. A. Auld, *Acoustic Fields and Waves in Solids* (Krieger, Malabar, Florida, 1990), Vol. II, pp. 77–83.
- [3] D. S. Potter and C. D. Leedham, *J. Acoust. Soc. Am.* **41**, 148 (1967).
- [4] J. Wolf, T. D. K. Ngoc, R. Kille, and W. G. Mayer, *J. Acoust. Soc. Am.* **83**, 122 (1987).
- [5] A. Alippi, M. Germano, A. Bettucci, F. Farrelly, and G. Muzio, *Phys. Rev. E* **57**, 4907 (1998).
- [6] A. Alippi, A. Bettucci, and M. Germano, *Ultrasonics* **38**, 817 (2000).
- [7] A. Alippi, A. Bettucci, and M. Germano, *Phys. Rev. E* **63**, 026604 (2001).
- [8] I. A. Viktorov, *Rayleigh and Lamb Waves* (Plenum Press, New York, 1967), pp. 83–93.
- [9] D. Royer and E. Dieulesaint, *Elastic Waves in Solids I* (Springer-Verlag, Berlin, 2000) pp. 49–60.